I.J. Image, Graphics and Signal Processing, **2025, 5, 62-75**
Published Online on October 8, 2025 by MECS Press (http://www.mecs-press.org/)
DOI: 10.5815/ijigsp.2025.05.05

Acne Types Prediction Using Acne Images based on Modified Link Net-B7 and HR-Net Algorithm

Priyanka R. Pandit*
KIT's College of Engineering, Kolhapur, Maharashtra-416234, India
E-mail: pandit.priyanka710@gmail.com
ORCID iD: https//orcid.org//0009-0004-6296-9359
*Corresponding Author

Mahesh S. Chavan
Department of Electronics & Telecommunication Engineering, KIT's College of Engineering, Kolhapur, Maharashtra-416234, India
Email: chavan.mahesh@kitcoek.in
ORCID iD: https//orcid.org//0000-0002-4847-0322

Received: 06 March, 2024; Revised: 15 July, 2024; Accepted: 11 May, 2025; Published: 08 October, 2025

Abstract: Acne is a persistent skin disorder that typically affects children in the age range of 12 to 25. Both inflammatory and non-inflammatory skin diseases can coexist with various types of acne, such as papules, pustules, nodules, cysts, blackheads, and whiteheads. In recent times, the study of acne has been carried out conventionally, with a manual approach for determining the ROI. As a result, the patient's face will be physically counted and marked with the acne that was found in the ROI. This manual method could result in incorrect identification and diagnosis of acne. Moreover, it is still difficult to determine the type of acne related to another. The necessity for patients to visit a dermatologist is growing despite the difficulties in identifying acne manually. For a patient, waiting for the dermatologist to become available is challenging. Thus, an automated application for recognizing acne types is needed, as it may help these individuals. In order to address these problems, a dataset containing images of skin diseases is created. Lanczos resampling, which is frequently used to shift or enhance a digital signal's sampling rate by a fraction of the sampling interval, is employed in the preprocessing of the skin disease data. Subsequently, the pre-processed images are segmented using the Modified Link Net-B7 in order to eliminate noise and correctly categorize images of acne with the segmented skin images. After the model has been trained and validated, the Acne type prediction is forecast using the HR-Net algorithm. The performance metrics for this developed model are FPR, FOR, NPV, kappa, error, accuracy, precision, sensitivity, specificity, f1-score, kappa, training time, testing time, and execution time. Performance metrics values of 95.17%, 94.10%, 92.33%, 96.34%, 93.15%, 85.74%, 4.83%, 4%, 6%, 95%, 7.7%, 1492, 23 and 1515 have been reached for the proposed approach. Therefore, compared to the existing models, Acne type prediction using the different types of Acne disease images based on modified Link Net-B7 and HR-Net algorithm performs better.

Index Terms: Acne Disease; Lanczos Resampling; Modified Link Net-B7; HR-Net Algorithm; Skin Disease

1. Introduction

In the medical field, automated evaluations of the severity of skin diseases are crucial. Common chronic inflammatory skin disease known as acne vulgaris affects the pilosebaceous units and is characterized by skin that is scarred, comedones, papules, nodules, pimples, and seborrhea [1]. Acne affects up to 650 million people globally, or 85% of teenagers as well as young adults. Acne is a skin condition that not only damages individuals physically but also significantly affects their mental health [2]. Low self-esteem, melancholy, worry, and even suicidal thoughts are frequently brought on by acne. Consequently, there's a big need for prompt and efficient acne treatment and diagnosis [3]. Dermatologists must evaluate the severity of the acne in order to choose the best course of action for a precise, uniform treatment. Global Acne Grading System (GAGS) as well as Hayashi criteria are commonly used by dermatologists as industry standards for severity [4]. In particular, there are four severity degrees for acne: mild, moderate, severe, and extremely severe. The conventional way of assessment involves seeing a dermatologist in the hospital to see and gauge the severity of acne. This process takes time and frequently depends on the dermatologist's experience [5]. In addition, patients frequently experience challenges with hospital registration, protracted hospital wait times, and poor access to transportation, particularly for those who reside in rural or impoverished areas. Sending images or videos to a dermatologist is another way to get advice on these matters, but dermatologists find that these technological transmission techniques take up time and may result in privacy difficulties. For this reason, an accurate and practical computer-aided diagnosis approach for acne is essential to its successful and efficient management [6].

Significant progress in the analysis of acne has been done in the last few years. Increasing popularity of convolutional neural network (CNN)-based techniques for diagnosing acne lesions can be attributed to deep learning's (DL) improved performance in image processing tasks [7]. A machine learning method to evaluate the severity of acne on the face, differentiate between lesions from comedoneal and inflammatory acne also identify residual or post-inflammatory hyperpigmentation (PIHP). CNN-based approaches are more versatile and perform better than most methods that rely on handcrafted features. However, there are still a few difficult issues when using CNNs to gauge the severity of acne [8]. First off, lesion type or amount alone is the basis for the widely used acne grading criteria. This is a poorly designed procedure that could lead to inaccurate grading outcomes from CNN-based systems. Second, it is challenging to differentiate between acne photos with equal severities due to their identical appearances. Adopting a deeper and wider network is a popular solution to this problem, However, it requires a lot of processing power (more potent GPUs) and isn't compatible with low-spec devices like smartphones. [9]. Additionally, rather than using patient data for a more individualized diagnosis, earlier research concentrated on making diagnoses based solely on images of acne. Therefore, it is a difficult task to obtain automated individualized assessments of acne severities that are independent of time and location [10].

Acne's clinical symptoms can take many different forms; comedones, papules, pustules, nodules, cysts, and more are common during adolescence and can last into adulthood. Nearly all teenagers between the ages of 15 and 17 get the illness, and it still affects 5% of women and 3% of men in their 40s and 49s. Acne has a significant negative psychological and economic impact [11]. The annual cost of treating acne and lost productivity in the United States alone exceeds $3 billion, placing a significant strain on the healthcare system. Adolescent patients experiencing physical changes as a result of acne are frequently depressed and socially isolated; also, delayed or ineffective therapy can cause major, irreversible harm to the patients' physical and mental well-being. Consequently, acne vulgaris treatment is very important for both individuals with the condition and society at large [12]. The management approach for acne is directly correlated with the assessment of its severity. At present, though, despite the availability of a wide range of techniques and standards for grading acne severity, the diagnosis and treatment selection are typically based more on the clinical experiences of the treating physician. Although becoming a certified dermatologist often requires extensive training, there are differences amongst dermatologists with regard to their clinical backgrounds [13]. Inadequate therapy for acne patients has been a result of both patient ignorance of the need for medical attention and patient accessibility to dermatologists, which both influence management strategies [14]. To overcome the abovementioned issues, Acne type's prediction using acne images based on modified Link Net-B7 and HR-Net algorithm. The main contributions of the proposed model are

- Acne type prediction using facial acne images based on modified Link Net-B7 and HR-Net algorithm.
- Collected Acne images are pre-processed using the Lanczos resampling for typically increase the sampling rate of a digital signal.
- Link Net-B7 technique is used for noise removal and segmenting the types of acne disease from the facial skin images.
- For training and classifying the types of acne from the segmented acne images, the HR-Net algorithm is used.

Paper's subsequent sections are organized as follows: Section 2 examines a number of publications on the prediction of acne disease type; Section 3 presented succinct description model is recommended. Section 4 presents experimental results for the constructed type of acne disease prediction model in addition to Section 5 concludes the study.

2. Literature Survey

Numerous methodologies established for the prediction of acne illness. The majority of the research papers have been analyzed, and some of them are reviewed below.

Farag et al. [15] developed a new ensemble learning technique for accurately identify and categorize acne in images using deep learning models. Prior to pruning the redundancy models based on model diversity and performance, it trains multi-base models. The foundation models that choose in the previous stage are then used to generate the extra properties of the training data. After that, it uses a feature selection technique to eliminate even more unnecessary models. In the end, all basic models are combined using classifiers. To reduce the size of the deep learning base models, an ensemble pruning technique was developed.

Alzahrani et al. [16] introduced Density maps were generated by a multi-scale dilated fully convolutional regressor in combination with an attention mechanism. The recommended fully convolutional regressor module systematically integrates multi-scale contextual information for the creation of density maps by adapting UNet with dilated convolution filters. To add an attention mechanism to the regressor model, it uses historical bounding box data produced by Faster R-CNN. By employing this attention process to identify the most significant characteristics linked to the understudied acne lesions, it was possible to increase the regressor model's resilience to a variety of facial acne lesion distributions in both sparse and dense areas. Ultimately, the number of acne lesions inside the image was calculated by integrating across the generated density maps; this number then indicates the severity of acne. Regression and classification metrics outperform state-of-the-art methods in the acquired results.

Huynh et al. [17] presented a Using facial image data from smartphones, an artificial intelligence system named AcneDet performs autonomous object detection and severity rating of acne. AcneDet has two models for the following two tasks: First, a LightGBM machine learning model that uses Investigator's Global Assessment (IGA) scale to determine the severity of acne; second, a Faster R-CNN-based deep learning model that can distinguish between four different types of acne lesion objects: papules/pustules, nodules/cysts, blackheads/whiteheads as well as acne scars. The LightGBM model was used to grade the severity of acne using the counts of each form of acne, which were the result of the Faster R-CNN model. For training, a dataset of 1572 tagged images of faces taken using both iOS and Android cell phones was utilized. According to the findings, the Faster R-CNN model detects acne objects with a mean accuracy of 0.54. The LightGBM model's average accuracy in assessing acne severity was 0.85.

Lin et al. [18] introduced and developed to create a single, universal framework for rating acne that can be applied to various grading criteria. It replicates, in two stages, the worldwide evaluation of the dermatologist's diagnosis. First, important information was enhanced and useless information was successfully filtered using an adaptive image pre-processing technique. Next, to mimic the dermatologists' comparison of local skin and global observation, an inventive network structure combines global deep features with local features. Furthermore, a transfer fine-tuning approach was suggested to move the previous understanding of one criterion to another, which effectively enhances the performance of the framework when there was inadequate data.

Kim et al. [19] used the genomic information of a relevant strain from ribotype 5, the virulent C. acnes genome-scale metabolic model (GEM), iCA843, was created in order to gain a thorough understanding of the pathogenic characteristics of C. acnes in the skin environment. In order to obtain qualitative model verification, it have to show that the model accurately anticipated the patterns of acetate and propionate formation, which agreed with the findings of the experiments. Furthermore, compared to other GEMWs of skin pathogens that cause acne, C. acnes was discovered to have distinct short-chain fatty acid production pathways. Constraint-based flow analysis with endogenous carbon sources in human skin revealed that a significant engagement of the Wood-Werkman cycle for NAD regeneration occurs in acne-associated skin diseases, leading to an elevated synthesis of propionate. Finally, it recommended possible targets for C. Acnes resistance utilizing a model-guided systematic method based on protein sequence similarity searches and gene essentiality analysis with a variety of skin microbiome species.

The majority of articles evaluated above are related to the type of acne disease prediction. It is usually necessary to combine numerous classifiers to ensure that the error converges to its asymptotic value. [15]. complexity of the traditional UNet architecture, which can affect training and accuracy [16]. It relatively computationally expensive compared to other object detection methods [17]. Complexity of computation [18]. When there is more noise in the data set, it performs poorly [19].

3. Proposed Methodology

Almost 80% of teenagers and young adults suffer from acne, a significant chronic inflammatory illness of the pilosebaceous unit, which includes the hair follicle, shaft, and sebaceous gland. Even when treated appropriately, it typically results in permanent disfigurement. Assessing risk factors for acne disease development in patients with acne disease and examining the relationship between these factors and the clinical features of the condition were the objectives of this study. The process flow of the proposed model is illustrated in Figure 1.

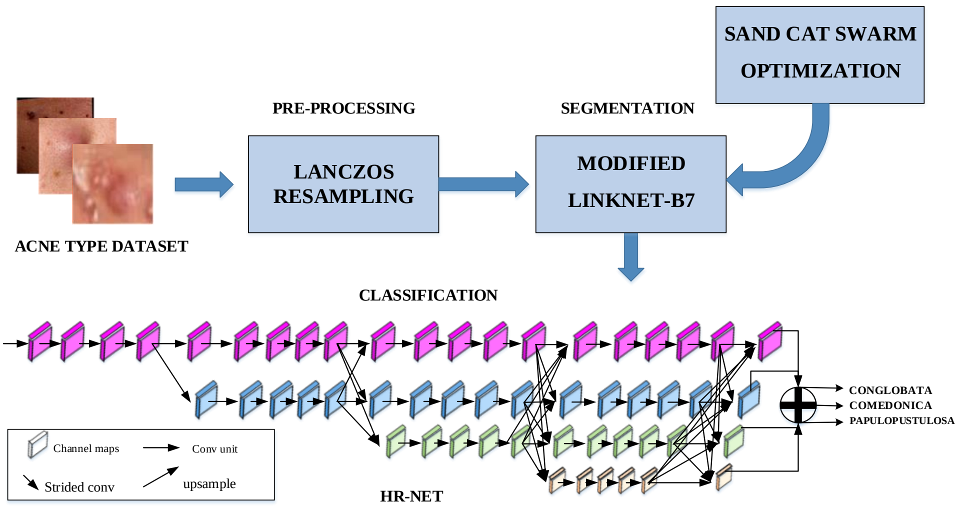

Fig. 1. Architecture for the Acne diseases in the Present Mode.

In this proposed model, the acne type disease dataset is collected and gathered as a dataset. These gathered facial images are preprocessed using Lanczos resampling to increase the sampling rate of a digital signal, or to shift it by a fraction of the sampling interval. Then, these pre-processed images are segmented using the Modified Link Net-B7 for removing the noise and segmentation of Acne disease images. After segmented images undergo the classification used in the HR-Net algorithm for predicting the type of acne disease, such as Conglobata, Comedonica Papulopustulosa.

3.1. Pre-Processing

A preliminary step is raw data analysis before moving on to the major phase or additional analysis. This pre-processing approach uses the Lanczos resampling algorithm.

3.1.1. Lanczos resampling

A method of scaling images called Lanczos resampling uses a kernel whose size is specified by a positive integer parameter, abbreviated as a. To get the best results, an is usually set to 2 or 3 [20]. In this instance, it selects a = 2, thus the kernel size in both the x and y Axes are 4 pixels. Consequently, to interpolate one pixel in the scaled image, a total kernel size of 4×4 is needed. The pixel values for the resulting image are interpolated by this algorithm using a sinc function as (1). This is how the Lanczos kernel is computed.

$$L(x) = \begin{cases} 1, & if\ x = 1 \\ \frac{a sin(\pi x)\sin(\pi x/a)}{\pi^2 x^2}, & if -a \leq x < a\ and\ x \neq 0 \\ 0, & otherwise \end{cases} \tag{1}$$

Equation (2) provides an interpolation formula that is used to carry out the interpolation calculations. Just two variables are used in this formula: x and i. If a pixel needs to be interpolated in either the x or y direction, its new position is represented by the variable x. The neighbouring pixel in the original image that corresponds to x is represented by i, on the other hand.

$$S(x) = \sum_{i=\lfloor x\rfloor-a+1}^{\lfloor x\rfloor+a} S_i L(x-i) \tag{2}$$

Pixel value $S(x)$ at the new position x in Equation (2) is determined by adding up the contributions of neighbouring pixels S_i and adjusting for weight using the Lanczos function $L(x - i)$. Using the distance between each neighboring pixel and the new position, the Lanczos function calculates each pixel's effect.

3.2. Segmentation

Image segmentation is a widely used method in digital image analysis as well as processing for dividing an image into different portions or areas, frequently depending on the properties of pixels in the image.

3.2.1. Modified Link Net-B7

Adam was found to be the optimizer [21]. Sigmoid was employed as the function for output. When there are two possible output classes, a sigmoid function is typically selected as the activation function for the output. Table 1 lists the specifications. The EfficientNet architecture relies on Mobile Inverted Bottleneck Convolution (MBConv), which is optimized for squeezing and excitation. The family of EfficientNet networks has various numbers of the MBConv blocks. From EfficientNetB0 to EfficientNetB7, the model's depth, width, resolution, and size grow while improving accuracy. The EfficientNetB7 model exceeds earlier CNNs in ImageNet accuracy, while simultaneously being 8.4-fold smaller and 6.1-fold faster. It is separated into seven blocks based on filter size, stride, and number of channels.

Table 1. Training Phase Parameters.

Parameter	**Noise Removal and Segmentation Phase**
Input size	256×256
Epoch number	5000
Optimizer	Adam
Batch size	8
Learning rate	0.001

Four encoder blocks and four decoder blocks are present. LinkNet was used for medical image segmentation due to its excellent accuracy and short epoch duration. EfficientNetB7 was employed as the encoder. This is because compared to other varieties, it has a higher accuracy and parameter count. It suggested LinkNet-B7, a LinkNet-based deep learning algorithm with an encoder of EquantNetB7 and an input size of 256 x 256 x 3. The encoder's structure is displayed in Table 2.

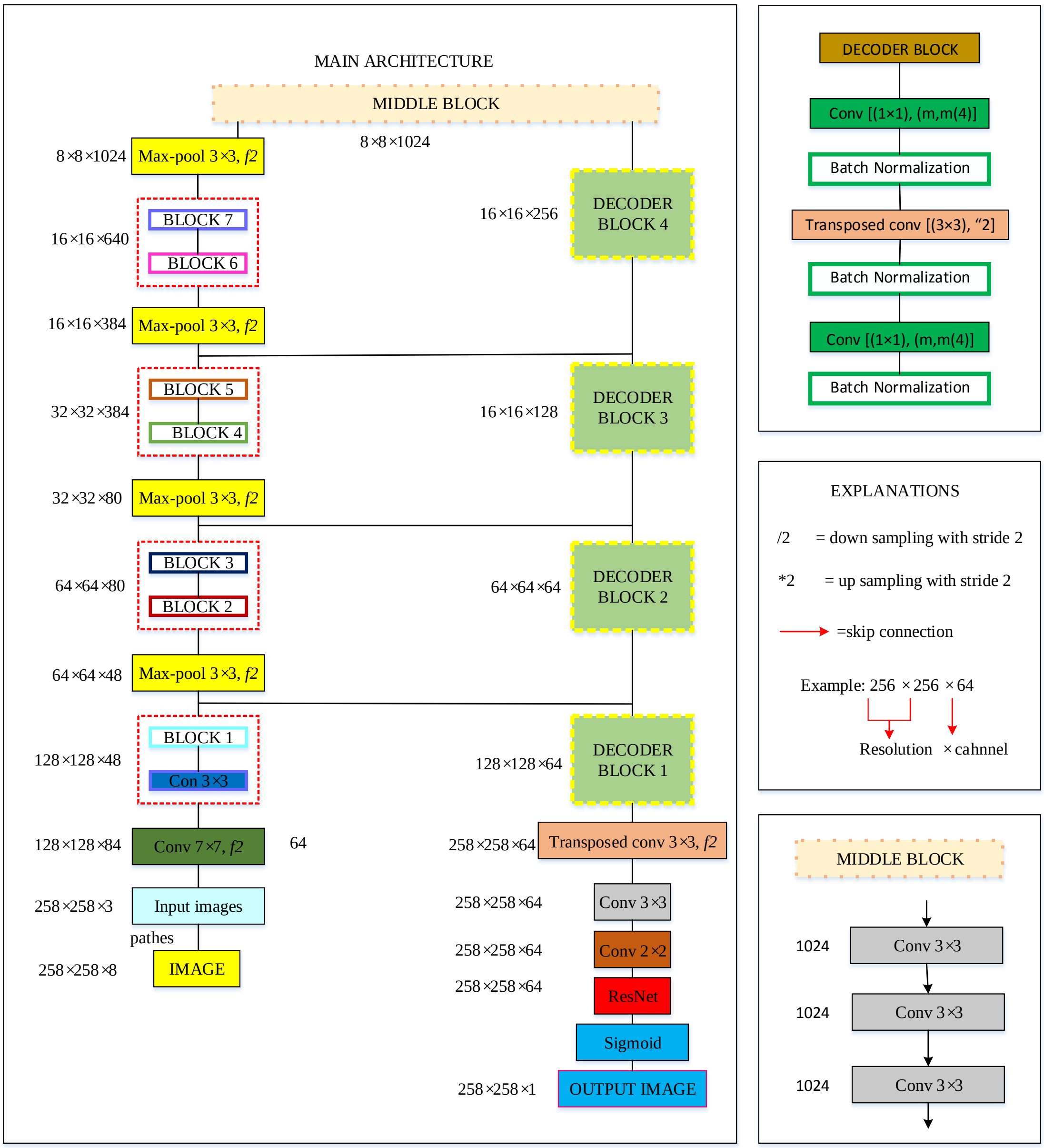

Fig. 2. LinkNet-B7 Architecture.

As other ResNet models include more layers, which slow down the model and increase the epoch time, our model included a single ResNet block before the last layer. Prior to the decoder blocks, it also used a middle block. By doing this, accuracy might be increased since it could gather more data before the decoder blocks.

Table 2. The encoder's structure.

Phase	Operator	Layers	Resolution	channels
1	Conv7× 7,/2	1	128 × 128	64
2	Conv3 × 3	1	128 × 128	64
3	Block 1-MBconv1 3 × 3	3	128 × 128	32
4	Block 2-MBconv1 3 × 3	7	64 × 64	48
5	Block 3-MBconv1 5 × 5	7	64 × 64	80
6	Block 4-MBconv1 3 × 3	10	32 × 32	80
7	Block 5-MBconv1 5 × 5	10	32 × 32	224
8	Block 6-MBconv1 5 × 5	13	16 × 16	384
9	Block 7-MBconv1 3 × 3	4	16 × 16	640

Finally, it made use of LinkNet-B7, a modified hybrid model. The input image is convoluted by the first block of the model using a 7x7 kernel with a stride of 2. This is followed by a max-pooling layer with a stride of 2. The model is shown in Figure 2.

3.2.2. Sand cat swarm optimization (SCSO)

The sand cats, who provided as the first source of inspiration for the suggested process, are discussed in this section [22]. Next, the suggested method's mathematical model and operation are explained.

Inspiration: Natural sand cats The Felis family of mammals includes the sand cat (Felis margarita) as one of its member species. Sand cats, which are adapted to harsh environments, can be found in stony and sandy deserts, including those found in central Asia, Africa, and the Arabian Peninsula. Small, agile also obedient, sand cats have distinctive lifestyles as well as hunting patterns. Even though there isn't much of an aesthetic distinction between sand cats and domestic cats, their lifestyles are very different. Sand cats don't live in a pack like many other cats do. Sand cats have fur on their palms too soles that is denser than normal, ranging from light grey to sandy. The fur on the soles of the feet shields the pads from the desert's intense heat and cold. Furthermore, the sand cat's hair is difficult to trace and detect. The sand cat's length ranges between 45 and 57 cm. Its tail (28-35 cm) is nearly half the length of its head and body, and its legs are small, as are its sharply curved border claws. The back claws are weakly curled and more extended when facing. The weight of an adult sand cat can vary from 1 to 3.5 kilograms. Ears are 5-7 centimetres long on either side of the head. The sand cat's ears are very important for foraging. This cat is unique because of its nocturnal, underground, and reclusive habits.

Sand Cat Swarm Optimization (SCSO) method was developed with inspiration from sand cat's natural behaviours. Sand cat's two main activities are hunting and foraging for food. The recommended strategy was modelled after the sand cat's special ability to recognize low frequency stimuli. The remarkable capacity of sand cats to locate prey on the ground as well as underground is impressive. This important feature allows it to find as well as seize its prey quickly. In order to emphasize the concept of swarm intelligence, developers of the proposed algorithm assumed that sand cats were a member of herds, despite the fact that they are solitary animals in the wild. The first stage in this method is to define the problem and create the initial population.

Step 1: Initialization

Hyper Parameters used for segmenting the acne type from the image are Batch size, Learning rate Epoch number, Input size and Optimizer are regarded as hyperparameters in LinkNet-B7. The below equation (3) represents the initialization of the hyperparameters for optimally selecting.

$$F = (X1, X2, \ldots., Xn) \tag{3}$$

Step 2: Fitness Function

Holdout cross-validation divides the entire dataset at random into a training and validation set. According to typical data partitioning standards, around 70% of the dataset will be used as a training set, with the remaining 30% serving as a validation set. The model is constructed only once on the training set and runs faster because the dataset is partitioned into only two sets.

$$fitness = \{maximize(acc_{cv})) \tag{4}$$

Step 3: Updating

Following Fitness function process, equation (5) is used to update every single other set of attributes. The optimization algorithm for the sand cat swarm determines the updating equation.

$$\overrightarrow{Pos}(t+1) = \vec{r}.\left(\left(\overrightarrow{Pos_{bc}}(t) - rand(0,1).\overrightarrow{Pos_c}(t)\right).\right. \tag{5}$$

Step 4: Termination

The entire process will be terminated after the LinkNet-B7 hyperparameters for effectively acquiring the data from the acne type illness images have been determined.

3.3. Classification

The High-Resolution Network was trained to predict Acne disease.

3.3.1. High-Resolution Network

High-resolution representations are maintained by the HRNet during the entire procedure [23]. It begins with a high-resolution convolution stream, adds convolution streams with progressively lower resolutions one by one, and then connects the multiple resolution streams in parallel. As shown in Figure 3, the final network is divided into multiple (four in the current design) stages, with the nth stage having n streams that correspond to n resolutions. It performs repeated multi-resolution fusions by repeatedly exchanging data across the parallel streams.

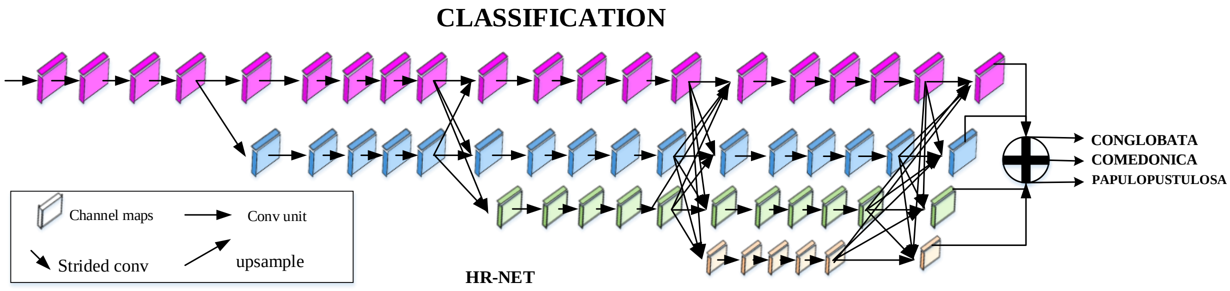

Fig. 3. Architecture of the designed HRNET.

The stem is not featured; only the main body is shown. There are four phases. Convolutions with great resolution make up the first level. Two-resolution (three-resolution, four-resolution) blocks are repeated multiple times (i.e., 1, 4, 3) in the second, third, and fourth stages.

In addition to being semantically robust, the high-resolution representations acquired from HRNet also exhibit exact spatial alignment. There are two sources for this. Firstly, instead of connecting high-to-low resolution convolution streams in series, our method does it in parallel. As a result, our method is able to preserve high resolution rather than restoring it from low resolution, and as a result, the learned representation has more spatial precision. The majority of fusion techniques now in use combine high-resolution low-level representations with up-sampled low-resolution high-level representations. Instead, it uses low-resolution representations to support high-resolution representations through multi-resolution fusions, and vice versa. All of the high-to-low resolution representations are therefore more semantically robust, which are combined together and based on the softmax layer the acne type classification has been done.

The model's ability to properly predict acne types including Conglobata, Comedonica, and Papulopustulosa has practical applications in dermatology. For example, severe forms like acne Conglobata frequently required system therapies such as isotretinoin, although lesser forms like Comedonica typically reacted well to topical retinoids. By giving an objective, consistent classification result, the system helped dermatologists choose the best treatment approach without the delays associated with manual diagnosis. This was especially useful in cases when access to dermatology specialists was limited or wait periods were lengthy. Furthermore, the system was integrated into follow-up protocols to track illness progression or treatment response over time, providing a quantitative and repeatable technique for assessing therapy efficacy. By minimizing diagnostic subjectivity and facilitating speedier decision-making, the model not only increased clinical workflow efficiency but also helped to reduce the psychological burden on patients, who frequently experienced discomfort as a result of delayed or wrong diagnosis. This improved explanation increased the clinical relevance of the research and linked technical achievements to actual gains in patient care.

4. Result and Discussion

Type of acne disease prediction using acne images based on modified Link Net-B7 and HR-Net algorithm. proThe specified model was implemented using a MATLAB program using the system CPU that included an Intel Core i7 processor and an NVIDA GeForce RTX 3070 GPU with 64GB of RAM. In this proposed methodology, Lanczos resampling is used to preprocess the obtained Acne disease datasets. The pre-processed images are then segmented using Modified Link Net-B7 and categorized using the HR-Net algorithm to forecast the kind of acne disease.

4.1. Dataset

Images were sourced from the publicly available Acne Type Classification v3 dataset on Roboflow Universe, which originally contained 754 images across 20 skin condition classes. For this study, only three clinically important acne types Acne Conglobata, Comedonica, and Papulopustulosa were selected, resulting in 726 images. The class distribution was outlined to ensure transparency[24]. All images were resized to 640×640 pixels and augmented using standard techniques to reflect varied imaging conditions. Bounding box annotations were provided through Roboflow’s platform, with a focus on maintaining dermatological accuracy. An 80/20 train-test split was used to ensure better test coverage than the dataset’s original split.

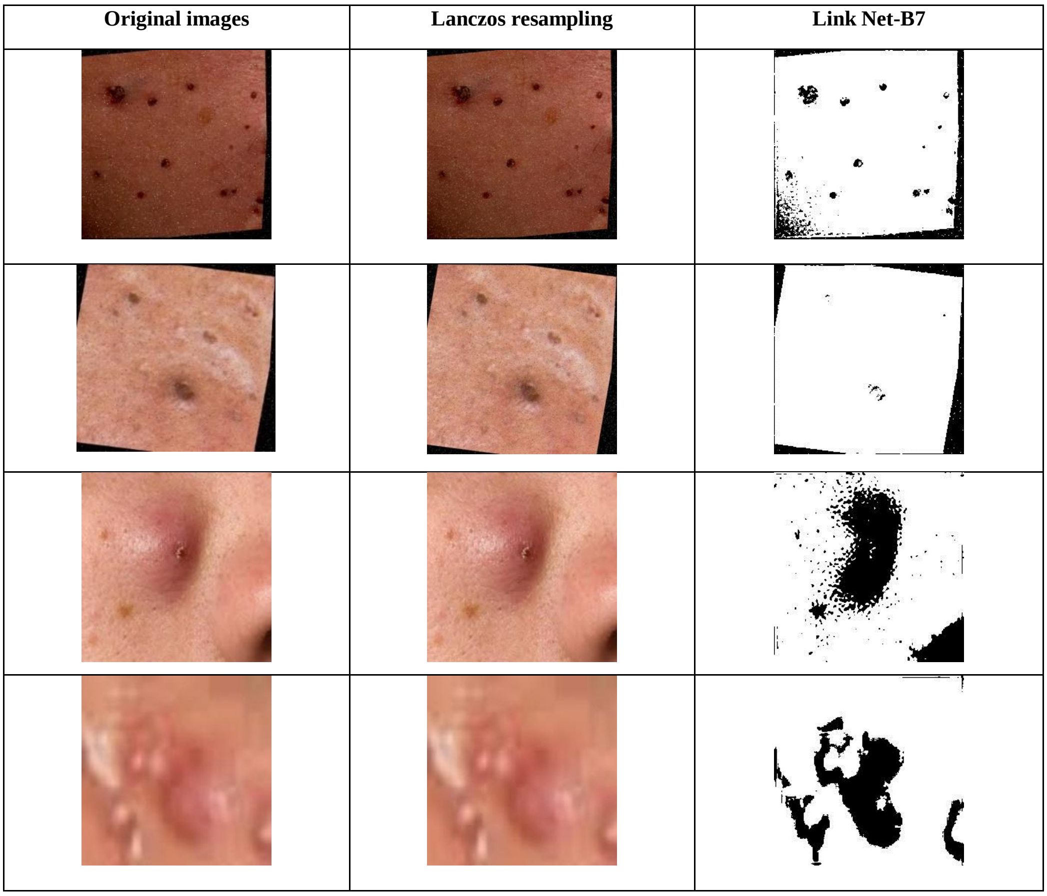

Fig. 4. Sample images using pre-processing and segmentation Model.

Figure 4 shows the transformation of Acne disease images utilizing segmentation by Modified Link Net-B7. Figure 4 shows the original image in the first column and the pre-processed type of the image in the second column. In the final column, segmented images are listed.

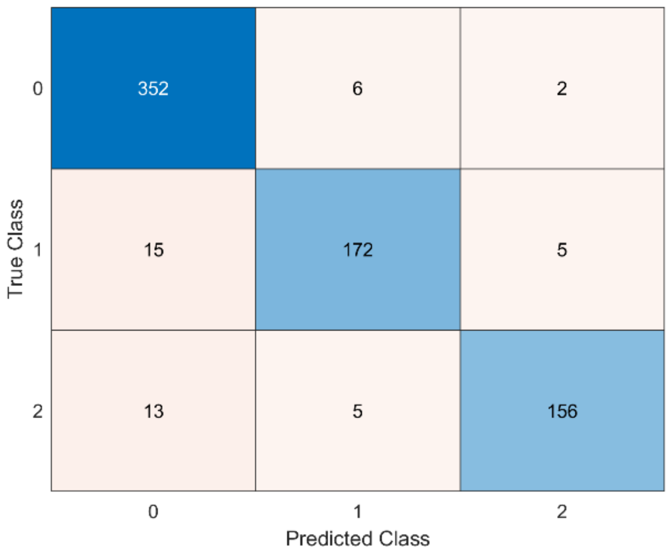

Fig. 5. Confusion Metrices in the Suggested Algorithm

Figure 5 demonstrates the confusion metrics in the proposed system. In this context having the three classes .The class 0 is Conglobata, class 1 is Comedonica, and class 2 is Papulopustulosa.

Table 3. Multi class classification based on confusion metrics.

	Predicted (0)	Predicted (1)	Predicted (2)
Actual (0)	TP=352	FP=6	FP=2
Actual (1)	FP=15	TP=172	FP=5
Actual (2)	FP=13	FP=5	TP=156

Examples of multiclass categorization's false positives and true positives are shown in Table 3. The column denotes the predicted(0), predicted(1),predicted(2) and the rows shows the actual(0),actual(1),actual(2).The values are showed in the predicted (0) is actual(0) the values is TP=352.

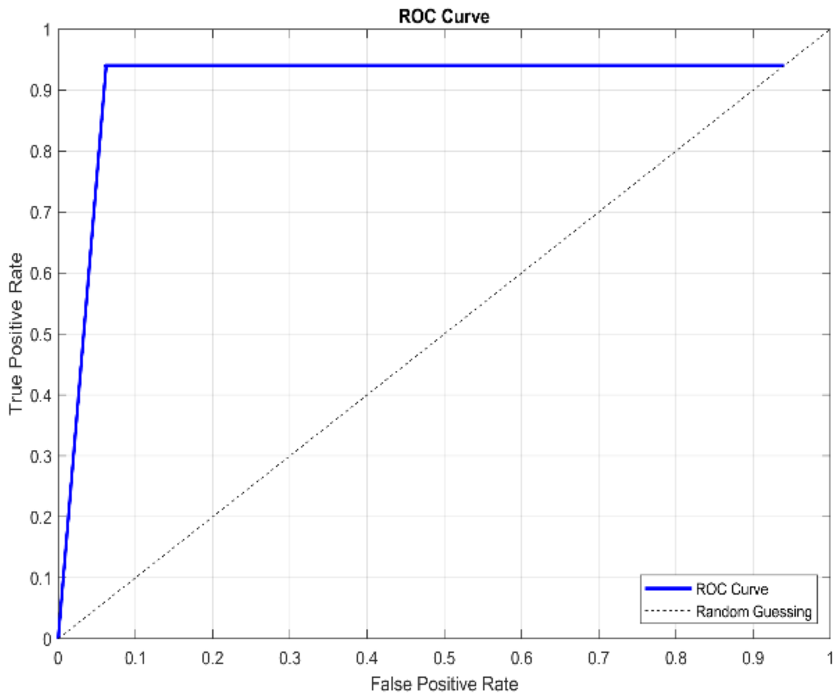

Fig. 6. ROC curve for the types of acne diseases.

Figure 6 shown in the ROC graph in the present model. In a graph, receiver operating characteristic curve (ROC) depicts the performance of the classification model for all thresholds. The area under the ROC curve, or AUC, measures the total two-dimensional region that lies beneath the complete ROC curve. Two variables, such as the true positive rate and false positive rate, are used to draw the curve.

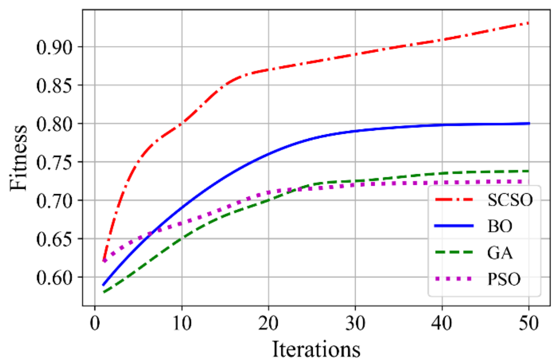

Fig. 7. Convergences Graph for the Optimization.

Figure 7 demonstrate the convergences plot for the suggested algorithm. Propoposed SCSO model converged faster at early iteration (15^{th}) while other existing algorithms such as BO, GA and PSO get converge later at 30^{th} and 35^{th} iteration. This shows improved performance of proposed optimization algorithm.

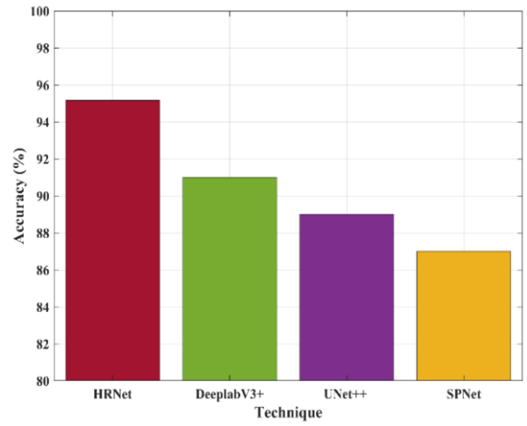
Accuracy (%)
HRNet
DeeplabV3+
UNet++
SPNet
Technique

(a)

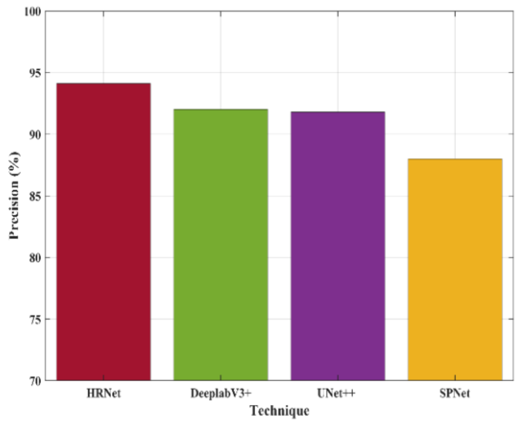
Precision (%)
HRNet
DeeplabV3+
UNet++
SPNet
Technique

(b)

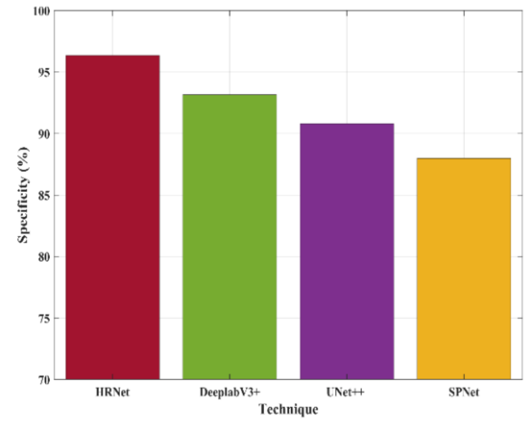
Specificity (%)
HRNet
DeeplabV3+
UNet++
SPNet
Technique

(c)

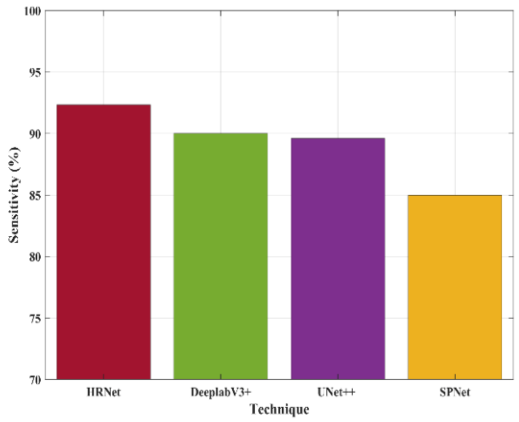
Sensitivity (%)
HRNet
DeeplabV3+
UNet++
SPNet
Technique

(d)

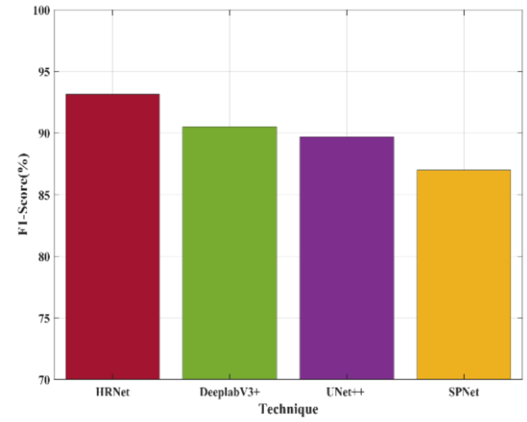
F1-Score(%)
HRNet
DeeplabV3+
UNet++
SPNet
Technique

(e)

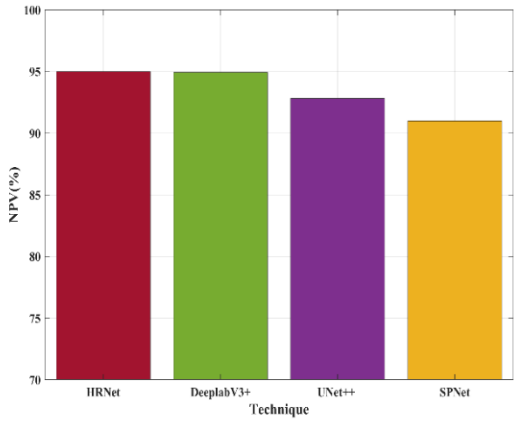
NPV(%)
HRNet
DeeplabV3+
UNet++
SPNet
Technique

(f)

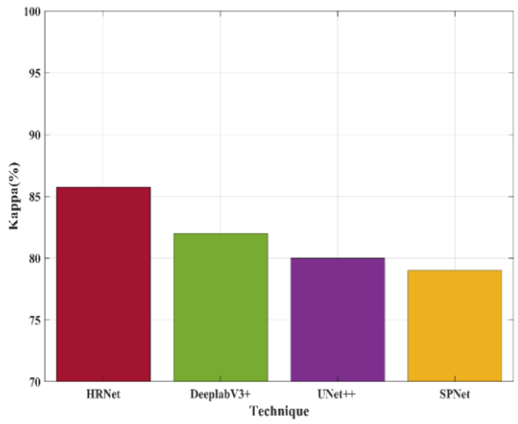
Kappa(%)
100
95
90
85
80
75
70
HRNet
DeeplabV3+
UNet++
SPNet
Technique

(g)

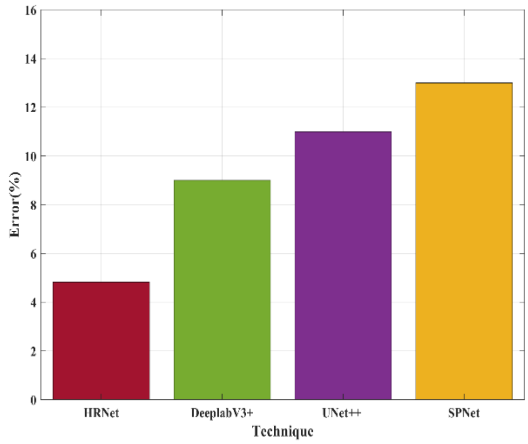
Error(%)
16
14
12
10
8
6
4
2
0
HRNet
DeeplabV3+
UNet++
SPNet
Technique

(h)

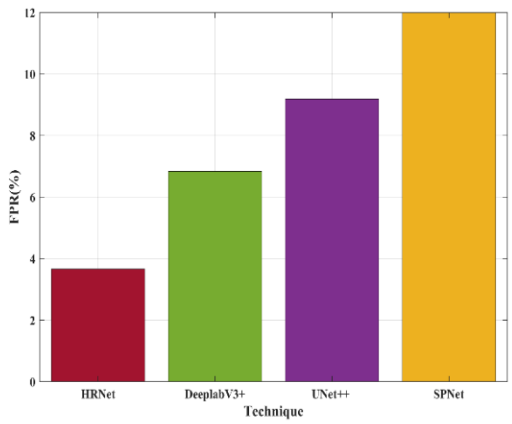
FPR(%)
12
10
8
6
4
2
0
HRNet
DeeplabV3+
UNet++
SPNet
Technique

(i)

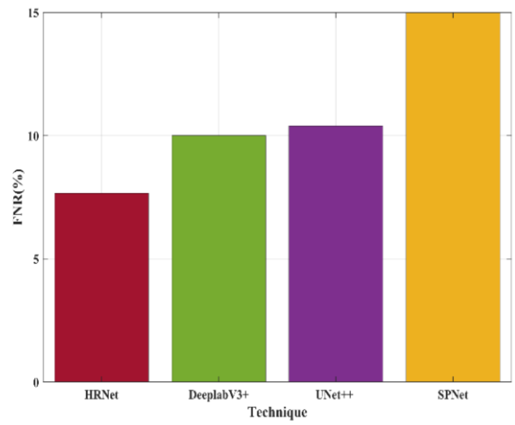
FNR(%)
15
10
5
0
HRNet
DeeplabV3+
UNet++
SPNet
Technique

(j)

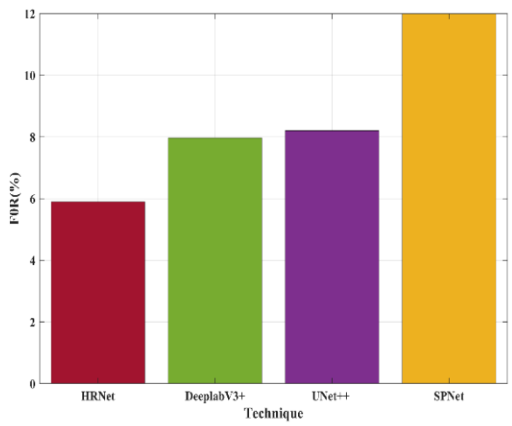
F0R(%)
12
10
8
6
4
2
0
HRNet
DeeplabV3+
UNet++
SPNet
Technique

(k)

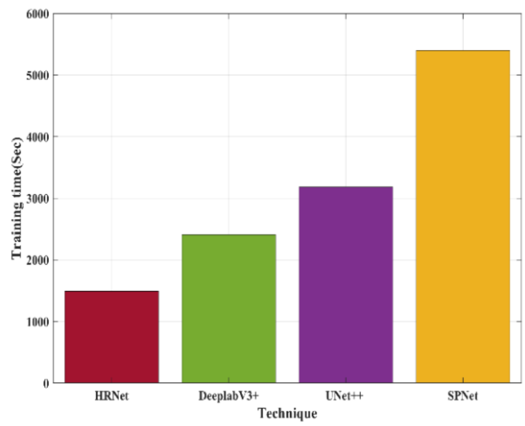
Training time(Sec)
6000
5000
4000
3000
2000
1000
0
HRNet
DeeplabV3+
UNet++
SPNet
Technique

(l)

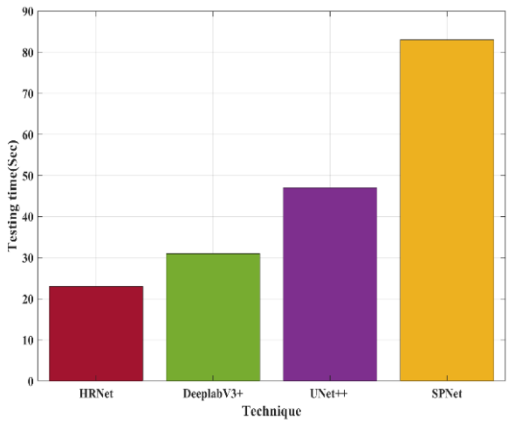

(m)

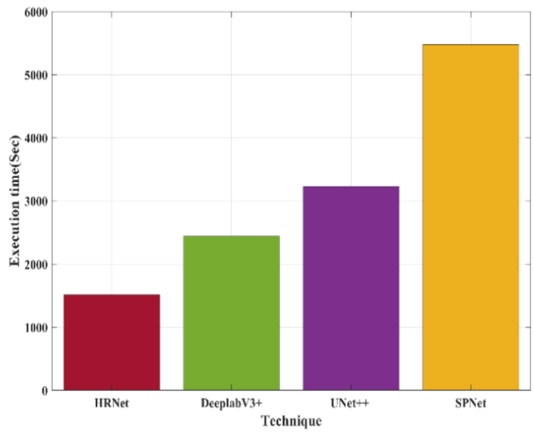

(n)

Fig. 8. Analysis for 8 a) Accuracy, b) Precision, c) Specificity, d) Sensitivity, e) F1-Score, f)NPV, g) Kappa, h) Error, i) FPR, j) FNR, k) F0R, l) Training Time(sec) , m) Testing Time(sec), n) Execution Time(sec)

Figure 8(a) illustrate between the proposed and exisiting model. The HR-Net values attained in 95.17% while the current model such as DeeplabV3+, Unet++ and SPNet the values is 95.17, 91, 89 and 87, respectively. Figure 8(b) denotes the precision. DeeplabV3+, Unet++ and SPNet is the various method. The proposed model is 94.10% in the precision values, Figure 8(c) compares the HR-Net with current model in specificity. The existing techniques like DeeplabV3+ is 93.16%, Unet++ is 90.18% and SPNet is 88%. While the HR-Net values are 96.34% respectively.

Figure 8(d) demonstrated the sensitivity for the HR-Net and existing model. Forecast is significantly impacted by the assumption (through its uncertainty and its model sensitivity) if the correlation coefficient between the assumption and the forecast is high. The proposed HR-Net and related model is 92.33 %, 90%, 89.6% and 85%. F1_score analysis in HR-Net and other model in Figure 8(e). The differences between the proposed and exisiting model the values is higher than the proposed model. The values in F1-Score is 93.15%. Figure 8(f) compares the HR-Net with the current algorithm in the NPV. The NPV values is high performed compared with the existing algorithm.

The Kappa comparison between the HR-Net and the existing methods is shown in Figure 8(g). The Kappa obtained for the HR-Net and other comparative values is 85.74% while the 82%,80% and 79%. HR-Net achieved the high level of the model. Figure 8(h) depicts the comparision of error metrices among HR-Net and other approaches.In this context context the error values is 4.83% in the proposed model. Additionally the exisiting model is high values.

Figure 8(i) and (j) represents the False Positive Rate and False Negative Rate . The FPR attained the value is 3.66%, 6.84%, 9.19%,12% in the HR-Net, DeeplabV3+, Unet++, and SPNet. While the FNR is 7.89% in the proposed model. Figure 8(k) denotes the false omission rate for each approach. The FOR values are 5.9 % for the HR-Net , 7.97% for DeeplabV3+,8.2 for Unet++ and 12 for SPNet.

Figure 8(l) compares the training time of HR-Net and other model. The HR-Net is 1492 seconds performs but the other model performed 2409 seconds , 3183 seconds and 5399 seconds respectively.This shows the HR-Net requires less time to train compared to the other. Figures 8 (m) and (n) presented the testing and overall execution time. The testing duration for DeeplabV3+, Unet++ and SPNet, the testing times attained are 23, 31, 47 and 83 seconds respectively. The total execution time for this model in 1515, 2440, 3230 and 5482. Based on this model HR-Net perform more efficiently.

5. Conclusion

An unwanted skin condition that affects the pilosebaceous unit is acne. The face, forehead, chest, upper back, and shoulders are the areas where it appears most frequently. Acne is typically associated with hormonal changes that occur during adolescence, yet some individuals (because of oil and dead skin cells) still have acne well into their 40s and 50s. Studies show that 40–50 million Americans suffer from acne and that about 80% of teenagers and young adults suffer from the condition. In addition to numerous other health issues, acne can cause pain, redness, and bleeding. For patients, the psychological and emotional consequences might be significantly more severe than the physical ones. The psychological issues that arise from changes in skin beauty include rage, despair, anxiety, fear, shame, embarrassment, low self-esteem, negative self-image, and others. Patients with acne may experience detrimental effects on their social lives as well, such as low self-esteem, less career opportunities, social disengagement, and in the worst cases, suicide thoughts. Here in this paper an acne disease dataset are collected and gathered as a dataset. Pre-processing of acne disease data involves the use of Lanczos resampling, which is commonly employed to enhance the digital signal's sampling rate or to move it by a portion of the sample interval. Following noise reduction and segmentation of the acne disease images using the Modified Link Net-B7, the pre-processed images are classified using the HR-Net algorithm to identify various types of acne disease. The performance metrics for this developed model are FPR, FOR, NPV, kappa, error, accuracy, precision, sensitivity, specificity, f1-score, kappa, training time, testing time, and execution time. Performance metrics values of 95.17%, 94.10%, 92.33%, 96.34%, 93.15%, 85.74%, 4.83%, 4%, 6%, 95%, 7.7%, 1492, 23 and 1515 have been reached for the proposed approach. Therefore, the efficacy of the updated Link Net-B7 and HR-Net algorithms for Acne disease prediction utilizing different types of Acne disease images is superior to that of the existing methods. This will help doctors and patients quickly treat skin conditions. There is access to research and minimal medical information implementation. The benefits of AI-assisted diagnosis can be investigated, as can the detection of acne disease, should more real-time data become available in the future.

Acknowledgement

Author contributions. The corresponding author claims the major contribution of the paper including formulation, analysis and editing. The co-author provides guidance to verify the analysis result and manuscript editing.

Compliance with ethical standards. This article is a completely original work of its authors; it has not been published before and will not be sent to other publications until the journal's editorial board decides not to accept it for publication.

References

[1] Z.V. Lim, F. Akram, C.P. Ngo, A.A. Winarto, W.Q. Lee, Liang, K., ... and H.K. Lee, "Automated grading of acne vulgaris by deep learning with convolutional neural networks," Skin Research and Technology, vol. 26, no. 2, pp. 187-192, 2020

[2] Y. Yang, L. Guo, Q. Wu, M. Zhang, R. Zeng, H. Ding,... and T. Lin, "Construction and evaluation of a deep learning model for assessing acne vulgaris using clinical images," Dermatology and Therapy, vol. 11, no. 4, pp. 1239-1248, 2021

[3] M.S. Junayed, M.B. Islam, A.A. Jeny, A. Sadeghzadeh, T. Biswas, and A.S. Shah, "ScarNet: development and validation of a novel deep CNN model for acne scar classification with a new dataset," IEEE Access, vol. 10, pp. 1245-1258, 2021

[4] N. Yadav, S.M. Alfayeed, A. Khamparia, B. Pandey, D.N. Thanh, and S. Pande, "HSV model‐based segmentation driven facial acne detection using deep learning," Expert Systems, vol. 39, no. 3, pp. e12760, 2022

[5] A. Sangha, and M. Rizvi, "Detection of acne by deep learning object detection," medRxiv, 2021-12, 2021

[6] H. Wang, J. Wang, M. Zhou, Y. Jia, M. Yang, and C. He, "Prediction of neonatal acne based on maternal lipidomic profiling," Journal of Cosmetic Dermatology, vol. 19, no. 10, pp. 2759-2766, 2020

[7] S. Karthick, and N. Muthukumaran, "Deep Regression Network for the Single Image Super Resolution of Multimedia Text Image," 2023 IEEE 5th International Conference on Cybernetics, Cognition and Machine Learning Applications (ICCCMLA), pp. 394-399, 2023 . Doi: 10.1109/ICCCMLA58983.2023.10346975

[8] H. Wen, W. Yu, Y. Wu, J. Zhao, X. Liu, Z. Kuang, and R. Fan, "Acne detection and severity evaluation with interpretable convolutional neural network models," Technology and Health Care, vol. 30, no. S1, pp. 143-153, 2022

[9] S. Karthick, and N. Muthukumaran, "U-Net Based Deep Regression Network Architecture for Single Image Super Resolution of License Plate Image," Lecture Notes in Networks and Systems, vol. 946, pp. 311-321, 2024. Doi: 10.1007/978-981-97-1323-3_26

[10] K.M. Monib, R.M. Salem, A.A. Alfallah, and S.E. EL-Sayed, "Risk Factors for Acne Vulgaris Development," Benha Journal of Applied Sciences, vol. 5(5 part (2)), pp. 283-287, 2020

[11] H. Zhang, and T. Ma, "Acne detection by ensemble neural networks. Sensors, vol. 22, no. 18, pp. 6828, 2022

[12] N.A.M. Isa, and N.N.A. Mangshor, "Acne type recognition for mobile-based application using YOLO," In Journal of Physics: Conference Series (Vol. 1962, No. 1, p. 012041), 2021. IOP Publishing.

[13] J. Zhang, L. Zhang, J. Wang, X. Wei, J. Li, X. Jiang, and D. Du, "Learning High-quality Proposals for Acne Detection," arXiv preprint arXiv:2207.03674, 2022

[14] S. Ibrahim, B. Osman, R.M. Awaad, and I. Abdoon, "Acne vulgaris relapse in sudanese patients treated with oral isotretinoin: Rate and predictive factors," Journal of Multidisciplinary Healthcare, pp. 839-849, 2023

[15] A.G. Farag, S.G. Helal, A.Z. Labib, and H.A. Bazid, "Study of calprotectin gene polymorphism and serum level in acne vulgaris patients," 2022

[16] S. Alzahrani, B. Al-Bander, and W. Al-Nuaimy, "Attention mechanism guided deep regression model for acne severity grading," Computers, vol. 11, no. 3, pp. 31, 2022

[17] Q.T. Huynh, P.H. Nguyen, H.X. Le, L.T. Ngo, N.T. Trinh, M.T.T. Tran,... and H.T. Ngo, "Automatic acne object detection and acne severity grading using smartphone images and artificial intelligence," Diagnostics, vol. 12, no. 8, pp. 1879, 2022

[18] Y. Lin, J. Jiang, Z. Ma, D. Chen, Y. Guan, H. You,... and G. Luo, "KIEGLFN: A unified acne grading framework on face images," Computer Methods and Programs in Biomedicine, vol. 221, pp. 106911, 2022

[19] S.K. Kim, M. Lee, Y.Q. Lee, H.J. Lee, M. Rho, Y. Kim,... and D.Y. Lee, "Genome-scale metabolic modeling and in silico analysis of opportunistic skin pathogen Cutibacterium acnes. Frontiers in Cellular and Infection Microbiology, vol. 13, 2023

[20] A. Sheibanifard, and H. Yu, "A Novel Implicit Neural Representation for Volume Data," Applied Sciences, vol. 13, no. 5, pp. 3242, 2023

[21] C. Akyel, and N. Arıcı, "LinkNet-B7: noise removal and lesion segmentation in images of skin cancer," Mathematics, vol. 10, no. 5, pp. 736, 2022

[22] A. Seyyedabbasi, and F. Kiani, "Sand Cat swarm optimization: A nature-inspired algorithm to solve global optimization problems," Engineering with Computers, vol. 39, no. 4, pp. 2627-2651, 2023

[23] Z. Zheng, S. Yu, and S. Jiang, "A domain adaptation method for land use classification based on improved HR-Net," IEEE Transactions on Geoscience and Remote Sensing, vol. 61, pp. 1-11, 2023

[24] Taschenbier (2023), Dataset link: https://universe.roboflow.com/taschenbier/acne-type-classification. Accessed on 12-02-2024.

Authors' Profiles

Ms. Priyanka Ramesh Pandit is a research student at KIT's College of Engineering, Kolhapur, India. Her research interests include artificial intelligence, deep learning, and medical image processing. She is focused on developing intelligent algorithms for healthcare diagnostics and image-based classification systems. With a strong foundation in computer vision and neural networks, she is dedicated to advancing practical AI applications in biomedical engineering and related fields.

Prof Mahesh Chavan is a Professor of Electronics and Telecommunication Engineering at Kolhapur Institute of Technology Kolhapur, India. He obtained his undergraduate degree in Electronics Engineering in 1991 from Shivaji University, India. He received his Master's Degree in Electrical Control Systems from Walchand college of Engineering Sangli, India. Prof Mahesh received his Ph.D. in Electronics and Communication from the Kurukshetra University Kurukshetra, India in 2009 under the joint supervision of the late Professor Ramawatar Agarawala from National Institute of Technology Kurukshetra India and Professor M.D. Uplane Department of Electronics Shivaji University Kolhapur. He has worked for his Post-Doctoral Research with Prof Nikos Mastorakis from Technical University of Sophia Bulgaria and published good research papers. He was appointed in the beginning of his career as teacher at the Department of Electronics Engineering at PVPIT Budhgaon in 1991 as a Lecturer. He was promoted to Senior lecturer in 1998. He was appointed as fulltime Professor in 2011 at Kolhapur Institute of Technology Kolhapur India. Prof Mahesh has made over 200 scholarly contributions, including nearly 125 peer-reviewed research papers (h-index = 16; i10-index = 24; with citations 1066, till date). He has published more than 100 papers in Scopus and SCI/UGC listed journals. He has received best research paper award in 2000 by IETE India. He has worked as reviewer in reputed peered reviewed journals and conferences. He has worked as technical Committee member in various reputed international Conferences. About 8 students have successfully completed their PhD under his supervision. He has guided more than 35 students for their Masters in Electronics Engineering and Electrical Engineering. Currently he is guiding about 8 students for their PhD and 3 students for their Masters. He has published about 6 patents along with his research students. He is member of various professional Bodies like ISTE, IETE, BIA, IEEE, WSEAS etc. Currently he is working as Steering Committee Member of Project CENTRAL funded by EU under Erasmus+ of 1,00,000 Euros as beneficiary. He has organized various international Workshops and National and international Conferences. He has worked as Member of Board of studies in Engineering of Shivaji University, Kolhapur India and Savitribai Phule Pune University, Pune India. He has worked as member board of studies at Shivaji University Kolhapur and Solapur University India. He has visited countries like Thailand, Turkey spain for attending conferences and Important meetings; workshops. He has received Individual credit mobility form European Commission. He has worked as Dean Academics at KIT and involved in various academic activities. He was fully active in implementing Academic Autonomy at KIT. He has initiated the process of implementing Curriculum through Project based Learning. His current research Interest is Signal Processing, Signal Behavior Study, and Biomedical Signal Processing.

How to cite this paper: Priyanka R. Pandit, Mahesh S. Chavan, "Acne Types Prediction Using Acne Images based on Modified Link Net-B7 and HR-Net Algorithm", International Journal of Image, Graphics and Signal Processing(IJIGSP), Vol.17, No.5, pp. 62-75, 2025. DOI:10.5815/ijigsp.2025.05.05